Towards a theory of self-organization phenomena in bubble-liquid mixtures

I. Akhatov
Department of Continuous Media Mechanics, Bashkir University, 32 Frunze Street, Ufa 450074, Russia

U. Parlitz and W. Lauterborn
Drittes Physikalisches Institut, Georg-August-Universität Göttingen, Bürgerstraße 42-44, D-37073 Göttingen, Germany
(Received 26 July 1995; revised manuscript received 27 June 1996)

A model for the theoretical description of one- and two-dimensional structure formation in bubble-liquid mixtures is developed. It consists of a coupled system of partial differential equations describing the spatiotemporal evolution of the sound field amplitude and the redistribution of bubbles in a liquid. A linear stability analysis of the (unstable) uniform bubble distribution is presented. Numerical simulations of the evolution of the sound field amplitude and the bubble concentration show self-organization phenomena. The relation between this system and the nonlinear Schrödinger equation is discussed. [S1063-651X(96)00311-X]

PACS number(s): 47.55.Bx, 43.25.+y, 43.35.+d

INTRODUCTION

Sound waves of high intensity propagating in a liquid give rise to the phenomenon of acoustic cavitation [1–5], whereby the liquid ruptures and forms cavities or cavitation bubbles. They group themselves in a remarkable way into a branched structure of filaments on a scale much smaller than the wavelength of the incident sound field. The filaments are called ''streamers'' in this context and the whole pattern ''acoustic Lichtenberg figures'' because of the striking similarity with the electrical discharge pattern obtained centuries ago by Lichtenberg [6,7]. Figure 1 gives an example of a bubble pattern as observed inside a cylindrical piezoelectric transducer operated in water at about 14 kHz.

A theoretical description of this phenomenon does not exist and a first step is presented here. The desired model has to incorporate self-organization properties and may be derived from the theory of wave propagation in liquids with bubbles [8–25] or from the dynamics of bubble clouds [27,28]. The most general and systematic approach to model wave phenomena in bubble-liquid mixtures has been done from the point of view of the mechanics of multiphase systems [12,13]. Here we are interested in the interaction of acoustic waves and quasistationary bubble-liquid mixtures.

This problem can be addressed at different levels of complexity. For instance, the sole action of the sound wave on the motion of bubbles or other particles may be considered to look into their slow motion under the influence of an acoustic field [13,17,18]. On the other hand, the sole action of the bubbles on a sound field may be studied giving shock waves and soliton alteration, self-focusing, self-transparency, modulational instability, difference frequency generation, etc. [19–26] (see also [1–5]).

In general, both the redistribution of the bubbles in the acoustic field and the influence of this redistribution on the acoustic wave have to be taken into account. This mutual interaction has been considered previously by Kobelev and Ostrovsky [29]. In their work, however, mainly the one-dimensional self-concentration of the bubbles in the propagation direction of the sound field has been investigated. For streamer formation, additionally the three-dimensional character of the phenomenon has to be taken into account: two dimensions in space and one dimension in time. This approach was presented in [30–32] for the two-dimensional case starting from plane acoustic waves in a homogeneous distribution of bubbles and investigating the stability of the configuration in the one-dimensional front of the wave. In that model the bubbles move to specific locations of the acoustic wave due to (primary) Bjerknes forces. This motion, however, changes the spatial distribution of bubbles in the wave front, which by itself has a strong influence on the sound field due to the dependence of the speed of sound on the bubble concentration.

In this paper a generalization of this theory is presented, taking into account the second dimension of the front and the influence of added mass forces on the motion of bubbles. In Sec. I the wave equation for bubble-liquid mixtures is derived and discussed. In Sec. II we derive a partial differential equation for the amplitude of the sound field that is essentially a nonlinear Schrödinger equation where the potential is replaced by the concentration of bubbles. The differential equation for the bubble concentration is derived in Sec. III. In Sec. IV boundary conditions and constants of motion are

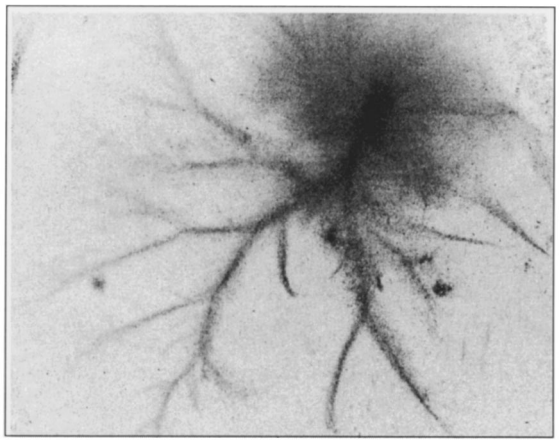

FIG. 1. Photograph of a bubble pattern as observed inside a cylindrical piezoelectric transducer of 7 cm inner diameter, driven at 14 kHz. (Courtesy of A. Billo.)

discussed. Section V contains a linear stability analysis for perturbations of plane waves that provides a criterion for a long-wavelength instability. The latter may be interpreted as the reason for the pattern formation as observed in the numerical simulations that will be presented in Sec. VI. The numerical methods used for solving our system of partial differential equations are briefly summarized in the Appendixes.

I. WAVE EQUATION FOR BUBBLE-LIQUID MIXTURES

In this section we follow [12,13] to derive the wave equation for a liquid containing gas bubbles. Let us consider the three-dimensional motion of an ideal weakly compressible liquid with a low-volume content of spherical gas bubbles of a given size. For simplicity thermal dissipation, capillary effects, and the coalescence and destruction of bubbles are neglected. Let α_l and α_g be the volume concentration, ρ_l and ρ_g the density, p_l and p_g pressure values of the liquid and the gas, respectively. Then the density ρ and the pressure p of the two-phase mixture are given by

$$\rho=\alpha_l\rho_l+\alpha_g\rho_g, \tag{1}$$

$$p=\alpha_l p_l+\alpha_g p_g, \tag{2}$$

where $\alpha_l+\alpha_g=1$. With $\rho_g \ll \rho_l$, $\alpha_g \ll 1$, and the assumption that all bubbles have the same radius R, we obtain the following approximations for the density and the pressure of the mixture:

$$\rho \simeq \rho_l(1-\alpha_g), \quad \alpha_g=\frac{4}{3}\pi R^3 N, \tag{3}$$

$$p \simeq p_l, \tag{4}$$

where N is the number of bubbles per unit volume of the mixture. The low compressibility of the liquid will be described by the linear (acoustic) approximation

$$\rho_l=\rho_{l0}+c_l^{-2}(p-p_0). \tag{5}$$

The subscript zero denotes the unperturbed state of the mixture and c_l is the velocity of sound in the pure liquid. Here and in the following we consider the polytropic equation for the gas inside the bubbles

$$p_g=p_0\left(\frac{R_0}{R}\right)^{3\kappa}, \tag{6}$$

where κ is the polytropic exponent ($\kappa=\gamma_g$ for adiabatic and $\kappa=1$ for isothermal oscillations of the bubbles, where γ_g denotes the gas adiabatic exponent). To analyze the combined deformation of liquid and gas it is necessary to use the Rayleigh equation for the radial motion of the liquid near the bubbles

$$\rho_l\left[R\frac{d^2R}{dt^2}+\frac{3}{2}\left(\frac{dR}{dt}\right)^2\right]=p_g-p, \quad \frac{d}{dt}=\frac{\partial}{\partial t}+(\mathbf{v}\cdot\nabla). \tag{7}$$

In this equation the pressure of the liquid p_l is replaced by the pressure of the mixture p [see Eq. (4)], d/dt is the substantial derivative, $\mathbf{v}$ equals the velocity of the mixture (liquid and bubbles move with equal velocities, i.e., we consider a single-velocity approximation) and the nabla operator is given by $\nabla=(\partial/\partial x,\partial/\partial y,\partial/\partial z)$. The equations for the number of bubbles, the mass of the mixture, and the equations of motion for the mixture are given by

$$\frac{\partial N}{\partial t}+\mathrm{div}(N\mathbf{v})=0, \tag{8}$$

$$\frac{\partial \rho}{\partial t}+\mathrm{div}(\rho\mathbf{v})=0, \tag{9}$$

$$\rho\frac{d\mathbf{v}}{dt}+\nabla p=\mathbf{0}. \tag{10}$$

Equations (3) and (5)–(10) completely describe the nonlinear nonstationary motion of the bubble-liquid mixture. To consider acoustic waves in such a system we linearize the system near the unperturbed state of the mixture and eliminate all variables except for the pressure.

For this purpose we introduce small perturbations p', ρ', $\mathbf{v}'$, N', and R' of the equilibrium values p_0, ρ_0, $\mathbf{v}_0=\mathbf{0}$, N_0, and R_0 such that $p=p_0+p'$, $\rho=\rho_0+\rho'$, $\mathbf{v}=\mathbf{v}'$, $N=N_0+N'$, and $R=R_0+R'$. From (3) and (5) we obtain

$$\rho=[\rho_{l0}+c_l^{-2}(p-p_0)]\left[1-\frac{4}{3}\pi R^3 N\right]. \tag{11}$$

Linearization yields

$$\rho'=\alpha_{l0}c_l^{-2}p'-\frac{4}{3}\pi R_0^3\rho_{l0}N'-4\pi R_0^2 N_0\rho_{l0}R', \tag{12}$$

where $\alpha_{l0}=1-\frac{4}{3}\pi R_0^3 N_0$ and $\rho_0=\rho_{l0}(1-\alpha_{g0})=\rho_{l0}\alpha_{l0}$. From Eqs. (6) and (7) we obtain

$$p=p_0\left(\frac{R_0}{R}\right)^{3\kappa}-\rho_l\left[R\frac{d^2R}{dt^2}+\frac{3}{2}\left(\frac{dR}{dt}\right)^2\right].$$

Linearization yields

$$p'=-\frac{3\kappa p_0}{R_0}R'-\rho_{l0}R_0\frac{\partial^2 R'}{\partial t^2}. \tag{13}$$

The linearizations of Eqs. (8), (9), and (10) are

$$\frac{\partial N'}{\partial t}+N_0\mathrm{div}(\mathbf{v}')=0, \tag{14}$$

$$\frac{\partial \rho'}{\partial t}+\rho_0\mathrm{div}(\mathbf{v}')=0, \tag{15}$$

$$\rho\frac{d\mathbf{v}'}{dt}+\nabla p'=\mathbf{0}. \tag{16}$$

Equations (14) and (15) yield

$$\frac{N'}{N_0}=\frac{\rho'}{\rho_0} \tag{17}$$

and from (15) and (6) one obtains

$$\frac{\partial^2 \rho'}{\partial t^2} = \Delta p'. \tag{18}$$

Substitution of (17) in (12) results in

$$\rho' = \alpha_{l0}^2 c_l^{-2} p' - 4\pi R_0^2 N_0 \rho_0 R', \tag{19}$$

which together with (13) yields

$$\left(\alpha_{l0} + \frac{\kappa p_0}{\alpha_{g0}\rho_{l0}} \alpha_{l0}^2 c_l^{-2} \right) p'$$

$$= \frac{\kappa p_0}{\alpha_{g0}\rho_{l0}} \rho' - \frac{R_0^2}{3\alpha_{g0}} \left(\alpha_{l0}^2 c_l^{-2} \frac{\partial^2 p'}{\partial t^2} - \frac{\partial^2 \rho'}{\partial t^2} \right). \tag{20}$$

If we differentiate this equation two times with respect to time and take into account Eq. (18), then we obtain the wave equation for a liquid containing gas bubbles in the form

$$\frac{\partial^2 p'}{\partial t^2} - c_0^2 \Delta p' + \frac{c_0^2}{\omega_r^2 c_\infty^2} \frac{\partial^2}{\partial t^2} \left(\frac{\partial^2 p'}{\partial t^2} - c_\infty^2 \Delta p' \right) = 0, \tag{21}$$

where

$$c_0^{-2} = c_\infty^{-2} + \frac{\rho_{l0}\alpha_{g0}}{\kappa p_0}, \quad c_\infty \simeq c_l,$$

$$\alpha_{g0} = \frac{4}{3}\pi R_0^3 N, \quad \omega_r^2 = \frac{3\kappa p_0}{\rho_{l0} R_0^2}. \tag{22}$$

Here ω_r is the resonance frequency of the bubbles. In Eqs. (21) and (22) α_{l0} is replaced by 1 because $\alpha_{g0} \ll 1$. The detailed analysis of Eq. (21) is given in [13,14].

It is easy to see that without gas bubbles ($\alpha_{g0}=0$, $R_0=0$) this equation reduces to the classical linear wave equation of acoustics. According to Eq. (21) the low-frequency waves ($\omega \ll \omega_r$) propagate with velocities that are close to c_0 and high-frequency waves possess a speed that converges to c_∞.

Taking into account that during the first stage of the cavitation process the bubbles are very small (microbubbles) and omitting dispersive effects we may use the low-frequency limit of the wave equation (21) in the form

$$\frac{\partial^2 p'}{\partial t^2} - c_0^2 \Delta p' = 0, \tag{23}$$

where the influence of the microbubble concentration is included in the velocity of sound c_0 [see Eq. (22)], which can be rewritten in the form

$$c_0^{-2} = c_l^{-2}(1 + \varepsilon n), \tag{24}$$

$$\varepsilon = \frac{c_l^2 \rho_{l0}}{\kappa p_0} \frac{4}{3}\pi R_0^3 N_*, \quad n = \frac{N}{N_*}. \tag{25}$$

Here N_* is some characteristic concentration of bubbles and n is the dimensionless concentration of bubbles. Here and in the following we will assume that n varies slowly in time and space.

II. EVOLUTION OF THE SOUND FIELD AMPLITUDE

For describing the evolution of the pressure amplitude p' ($p' = p - p_0$) of the sound field we start with the three-dimensional wave equation

$$c_0^{-2} \frac{\partial^2 p'}{\partial t^2} = \frac{\partial^2 p'}{\partial x^2} + \frac{\partial^2 p'}{\partial y^2} + \frac{\partial^2 p'}{\partial z^2}, \tag{26}$$

where c_0, the speed of sound in the mixture, is given by Eq. (24). The parameter ε is small and of the order of 10^{-2}. If we assume the following values for the physical parameters: $c_l \sim 10^3$ m/s, $\rho_{l0} \sim 10^3$ kg/m^3, $\kappa \sim 1$, $p_0 \sim 10^5$ N m^{-2}, $R_0 \sim 10^{-5}$ m, and $N_* \sim 10^9$ m^{-3}, we obtain, for example, $\varepsilon = 0.04$.

Let us consider the stability of plane acoustic waves that propagate along the z axis. In the case $\varepsilon = 0$ the exact solution of Eq. (26) for the wave propagation process may be written as

$$p' = \frac{1}{2} \left\{ W_0 \exp\left[i\omega \left(t - \frac{z}{c_l} \right) \right] + \text{c.c.} \right\}, \tag{27}$$

where W_0 is the constant complex wave amplitude and c.c. denotes the complex conjugate. For the stability analysis we consider perturbations of W_0 in the front of the plane wave. Therefore we approximate the solution of Eq. (26) in the form

$$p' = \frac{1}{2} \left\{ W(T,X,Y) \exp\left[i\omega \left(t - \frac{z}{c_l} \right) \right] + \text{c.c.} \right\}, \tag{28}$$

where $T = \varepsilon t$, $X = \sqrt{\varepsilon} x$, and $Y = \sqrt{\varepsilon} y$ are slow variables. Substituting the derivatives

$$\frac{\partial^2 p'}{\partial x^2} = \frac{\varepsilon}{2} \left\{ \frac{\partial^2 W}{\partial X^2} \exp\left[i\omega \left(t - \frac{z}{c_l} \right) \right] + \text{c.c.} \right\}, \tag{29}$$

$$\frac{\partial^2 p'}{\partial y^2} = \frac{\varepsilon}{2} \left\{ \frac{\partial^2 W}{\partial Y^2} \exp\left[i\omega \left(t - \frac{z}{c_l} \right) \right] + \text{c.c.} \right\}, \tag{30}$$

$$\frac{\partial^2 p'}{\partial z^2} = -\left(\frac{\omega}{c_l} \right)^2 \frac{1}{2} \left\{ W \exp\left[i\omega \left(t - \frac{z}{c_l} \right) \right] + \text{c.c.} \right\}, \tag{31}$$

$$\frac{\partial^2 p'}{\partial t^2} = \frac{1}{2} \left\{ \left(\varepsilon^2 \frac{\partial^2 W}{\partial T^2} + 2i\omega\varepsilon \frac{\partial W}{\partial T} - \omega^2 W \right) \times \exp\left[i\omega \left(t - \frac{z}{c_l} \right) \right] + \text{c.c.} \right\} \tag{32}$$

in Eq. (26) and neglecting the terms proportional to ε^2 yields, with Eq. (24),

$$\frac{2i\omega}{c_l^2} \frac{\partial W}{\partial T} = \frac{\partial^2 W}{\partial X^2} + \frac{\partial^2 W}{\partial Y^2} + \left(\frac{\omega}{c_l} \right)^2 n W. \tag{33}$$

If we use the dimensionless variables ξ, η, ζ, and w,

$$\xi = \frac{1}{2}\omega T = \frac{1}{2}\omega\varepsilon t, \quad \eta = \frac{\omega}{c_l} X = \frac{\omega}{c_l}\sqrt{\varepsilon} x,$$

$$\zeta=\frac{\omega}{c_l}Y=\frac{\omega}{c_l}\sqrt{\varepsilon}y, \quad w=\frac{W}{W_*}, \tag{34}$$

we obtain the amplitude equation in the form

$$i\frac{\partial w}{\partial \xi}=\frac{\partial^2 w}{\partial \eta^2}+\frac{\partial^2 w}{\partial \zeta^2}+nw. \tag{35}$$

Equation (35) is a nonlinear Schrödinger equation with the potential being replaced by the concentration of bubbles n.

III. EVOLUTION OF THE BUBBLE CONCENTRATION IN THE SOUND FIELD

All bubbles with volume V_g experience a force

$$\mathbf{F}=-V_g\nabla p, \tag{36}$$

where ∇p is the pressure gradient. If p and V_g vary in time with high frequency it is possible to calculate the time average of the force. This primary Bjerknes force [33,34] can be written as

$$\mathbf{F}_B=-\langle V_g(t)\nabla p(x,y,z,t)\rangle, \tag{37}$$

where the angular brackets denote the time average (over one period $2\pi/\omega$ of the oscillation of p). In our case, the pressure field may be described by

$$\begin{aligned} p&=p_0+\frac{1}{2}\left\{(W_R+iW_I)\exp\left[i\omega\left(t-\frac{z}{c_l}\right)\right]\right. \\ &\left.+(W_R-iW_I)\exp\left[-i\omega\left(t-\frac{z}{c_l}\right)\right]\right\} \\ &=p_0+W_R\cos\left[\omega\left(t-\frac{z}{c_l}\right)\right]-W_I\sin\left[\omega\left(t-\frac{z}{c_l}\right)\right], \end{aligned} \tag{38}$$

where

$$W(\xi,\eta,\zeta)=W_R(\xi,\eta,\zeta)+iW_I(\xi,\eta,\zeta). \tag{39}$$

Now we shall consider a bubble located at the point (x,y,z) in the acoustic field and oscillating far below its resonance frequency ω_r. For small deviations $R'=R-R_0$ of the radius of the bubble R from its value at equilibrium R_0 we obtain the equation of motion

$$\begin{aligned} \ddot{R}'+\omega_r^2R'=&-\frac{1}{\rho_{l0}R_0}\left\{W_R(\xi,\eta,\zeta)\cos\left[\omega\left(t-\frac{z}{c_l}\right)\right]\right. \\ &\left.-W_I(\xi,\eta,\zeta)\sin\left[\omega\left(t-\frac{z}{c_l}\right)\right]\right\}. \end{aligned} \tag{40}$$

The solution of this equation is

$$\begin{aligned} R'=&-\frac{1}{\rho_{l0}R_0(\omega_r^2-\omega^2)}\left\{W_R(\xi,\eta,\zeta)\cos\left[\omega\left(t-\frac{z}{c_l}\right)\right]\right. \\ &\left.-W_I(\xi,\eta,\zeta)\sin\left[\omega\left(t-\frac{z}{c_l}\right)\right]\right\} \end{aligned} \tag{41}$$

because W_R and W_I are functions that change slowly in time and space. Then the oscillations of the bubble volume are given by

$$\begin{aligned} V_g(t)&=\frac{4}{3}\pi R^3(t)=\frac{4}{3}\pi R_0^3\left[1+\frac{R'(t)}{R_0}\right]^3 \\ &\approx V_{g0}\left(1+\frac{3}{R_0}R'(t)\right) \\ &=V_{g0}\left(1-\frac{3}{\rho_{l0}R_0^2(\omega_r^2-\omega^2)}\right. \\ &\quad\times\left\{W_R(\xi,\eta,\zeta)\cos\left[\omega\left(t-\frac{z}{c_l}\right)\right]\right. \\ &\quad\left.\left.-W_I(\xi,\eta,\zeta)\sin\left[\omega\left(t-\frac{z}{c_l}\right)\right]\right\}\right). \end{aligned} \tag{42}$$

The pressure gradient $\nabla p=(\partial p/\partial x,\partial p/\partial y,\partial p/\partial z)$ is given by

$$\begin{aligned} \frac{\partial p}{\partial x}&=\frac{\omega}{c_l}\sqrt{\varepsilon}\left\{\frac{\partial W_R}{\partial \eta}\cos\left[\omega\left(t-\frac{z}{c_l}\right)\right]-\frac{\partial W_I}{\partial \eta}\sin\left[\omega\left(t-\frac{z}{c_l}\right)\right]\right\}, \\ \frac{\partial p}{\partial y}&=\frac{\omega}{c_l}\sqrt{\varepsilon}\left\{\frac{\partial W_R}{\partial \zeta}\cos\left[\omega\left(t-\frac{z}{c_l}\right)\right]-\frac{\partial W_I}{\partial \zeta}\sin\left[\omega\left(t-\frac{z}{c_l}\right)\right]\right\}, \\ \frac{\partial p}{\partial z}&=\frac{\omega}{c_l}\left\{W_R\sin\left[\omega\left(t-\frac{z}{c_l}\right)\right]+W_I\cos\left[\omega\left(t-\frac{z}{c_l}\right)\right]\right\}. \end{aligned} \tag{43}$$

If we insert Eqs. (42) and (43) into Eq. (37) and average over one period $2\pi/\omega$, we obtain the primary Bjerknes force

$$\mathbf{F}_B=\left(\gamma_1\frac{\partial(|W|^2)}{\partial \eta},\gamma_1\frac{\partial(|W|^2)}{\partial \zeta},0\right),$$

$$\gamma_1=\frac{3V_{g0}}{4\rho_{l0}R_0^2(\omega_r^2-\omega^2)}\frac{\omega}{c_l}\sqrt{\varepsilon}. \tag{44}$$

The interaction forces between the liquid and the bubbles include also the Stokes (friction) force $\mathbf{F}_S$ and the added mass force $\mathbf{F}_M$. Taking into account that the temporally averaged motion of the bubbles is slow and that the shape of the bubbles is spherical, the simplest formulas for the forces $\mathbf{F}_S$ and $\mathbf{F}_M$ are

$$\mathbf{F}_S=-6\pi\mu_l R_0\mathbf{U}, \tag{45}$$

$$\mathbf{F}_M=-\frac{1}{2}\rho_{l0}V_{g0}\frac{\partial \mathbf{U}}{\partial \mathbf{t}}, \tag{46}$$

where $\mathbf{U}=(U_x,U_y,0)$ is the velocity vector describing the slow displacement of the bubbles and μ_l is the viscosity of the liquid. Then the equation for slow drift of bubbles in the liquid is

$$\mathbf{F}_B+\mathbf{F}_S+\mathbf{F}_M=\mathbf{0}. \tag{47}$$

From this equation one can derive an equation for the evolution of the velocity of the bubbles in the form

$$T_2\frac{\partial\mathbf{U}}{\partial t}+\mathbf{U}=\Gamma\boldsymbol{\nabla}_{\eta\zeta}|W|^2, \tag{48}$$

with

$$T_2=\frac{\rho_{l0}V_{g0}}{12\pi\mu_l R_0},\quad \Gamma=\frac{\gamma_1}{6\pi\mu_l R_0}, \tag{49}$$

where $\boldsymbol{\nabla}_{\eta\zeta}=(\partial/\partial\eta,\partial/\partial\zeta,0)$ and T_2 is a characteristic time for the relaxation of the velocity of the bubbles. If we use the dimensionless variables η,ζ,w [see Eq. (34)], and

$$\mathbf{u}=\frac{\mathbf{U}}{U_*},\quad U_*=\frac{c_l}{2}\sqrt{\varepsilon},\quad \gamma=\frac{\Gamma W_*^2}{U_*},\quad \tau_2=\frac{1}{2}\omega T_2\varepsilon, \tag{50}$$

we obtain a relaxational equation for velocity in the form

$$\tau_2\frac{\partial\mathbf{u}}{\partial\xi}+\mathbf{u}=-\gamma\nabla_{\eta\zeta}(|w|^2). \tag{51}$$

Using the dimensionless variables of Eqs. (34), (25), and (50) it is possible to rewrite the conservation law for the bubble concentration during the slow redistribution of bubbles in space,

$$\frac{\partial N}{\partial t}+\mathrm{div}(N\mathbf{U})=0, \tag{52}$$

in the form

$$\frac{\partial n}{\partial\xi}+\frac{\partial(nu_x)}{\partial\eta}+\frac{\partial(nu_y)}{\partial\zeta}=0, \tag{53}$$

with $\mathbf{u}=(u_x,u_y,0)$.

It is well known that microbubbles cannot exist for a long time without an acoustic field (see [35]). Applying theoretical results [36], one can show that air bubbles in water with a size of a few micrometers will dissolve in a few seconds. Let us assume that the volume of the bubbles decreases exponentially in time. Since we consider only bubbles of fixed size this effect is taken into account by an exponentially decreasing number of bubbles that is given by the differential equation

$$\frac{\partial N}{\partial t}=-\frac{N}{T_1}, \tag{54}$$

where T_1 is the characteristic time of dissolution of microbubbles.

When an acoustic field of sufficiently high amplitude is switched on, it may stop the dissolution and support the formation of microbubbles. It is easy to estimate [13] that for small amplitudes of the acoustic field the energy flow into the bubble for one period of oscillations is directly proportional to the square of the pressure amplitude of the external field. Therefore, the concentration of generated bubbles should be directly proportional to the energy of the acoustic field $|W|^2$. When increasing the amplitude of the acoustic field the concentration of generated bubbles converges to some saturation value N_∞, which describes the limited amount of gas diluted in the liquid. This fact can be phenomenologically taken into account by including an additional term

$$F(|W|^2)=N_\infty\left[1-\exp\left(-\frac{\delta|W|^2}{N_\infty}\right)\right] \tag{55}$$

in Eq. (54) to describe the generation of bubbles by the acoustic field where the parameter δ controls the generation of bubbles. Then Eq. (54) can be written as

$$\frac{\partial N}{\partial t}=-\frac{N-F(|W|^2)}{T_1}. \tag{56}$$

It should be emphasized that for the derivation of Eq. (56) effects connected with threshold phenomena have been omitted (e.g., the quasistatic Blake threshold pressure [37]), because the main aim of the present paper is to investigate the self-organizing behavior of bubble fields above the cavitation threshold.

Adding the concentration growth and decay term of Eq. (56) to Eq. (52) yields the desired partial differential equation for the evolution of the bubble concentration in a sound field. Choosing as normalizing constant $N_*=\delta|W_*|^2$, the dimensionless form of this equation may be written as

$$\frac{\partial n}{\partial\xi}+\frac{\partial(nu_x)}{\partial\eta}+\frac{\partial(nu_y)}{\partial\zeta}=-\frac{n-f(|w|^2)}{\tau_1}, \tag{57}$$

$$f(|w|^2)=A_\infty^2[1-\exp(-|w|^2/A_\infty^2)],$$

where

$$\tau_1=\frac{\omega\varepsilon}{2}T_1 \tag{58}$$

and

$$A_\infty^2=\frac{N_\infty}{N_*}. \tag{59}$$

The parameter τ_1 is difficult to estimate exactly. In any case, however, T_1 has to be much larger than the period $2\pi/\omega$ of the acoustic oscillation. Finally, we want to note that for $\tau_1=0$ and $A_\infty\to\infty$ Eq. (57) implies $n=|w|^2$ and therefore Eq. (35) becomes the ordinary nonlinear Schrödinger equation

$$i\frac{\partial w}{\partial\xi}=\frac{\partial^2 w}{\partial\eta^2}+|w|^2w. \tag{60}$$

IV. BOUNDARY CONDITIONS AND CONSTANTS OF MOTION

The boundary conditions for the amplitude w,

$$\frac{\partial w}{\partial \eta}(0,\zeta,\xi)=\frac{\partial w}{\partial \eta}(L_x,\zeta,\xi)=0 \tag{61}$$

and

$$\frac{\partial w}{\partial \zeta}(\eta,0,\xi)=\frac{\partial w}{\partial \zeta}(\eta,L_y,\xi)=0, \tag{62}$$

describe the reflection from the lateral walls of the channel where L_x and L_y are the dimensionless distances between the walls. It is easy to show that the energy of the sound field

$$E(\xi)=\int_0^{L_x}\int_0^{L_y}|w(\eta,\zeta,\xi)|^2 d\eta d\zeta \tag{63}$$

is a constant of motion that depends only on the initial distribution of the amplitude $w=w(\eta,\zeta,0)$. For $A_\infty\to\infty$ the temporal evolution of the total number of bubbles

$$M(\xi)=\int_0^{L_x}\int_0^{L_y} n(\eta,\zeta,\xi) d\eta d\zeta \tag{64}$$

can be described by the ordinary differential equation

$$\frac{\partial M}{\partial \xi}=\frac{E-M}{\tau_1}. \tag{65}$$

This equation is obtained by integrating Eq. (57) in space, taking into account the boundary conditions for the velocity components

$$u_x(0,\xi)=0=u_x(L_x,\xi),\ \ u_y(0,\xi)=0=u_y(L_y,\xi). \tag{66}$$

When the initial distribution of bubbles $n(\eta,0)$ is chosen to be equal to the initial energy density of the acoustic field $|w(\eta,\zeta,0)|^2$, then $M(0)=E(0)=E_0$ and the total number of bubbles M has to be constant in time $M(\xi)=E_0$. This fact has been used for controlling the accuracy of the numerical method. For all results presented in this paper the deviation of E and M from their initial values was smaller than 1%. If $M(0)$ is different from E_0 then $M(\xi)$ converges to this stable equilibrium value, as can be seen directly from Eq. (65).

V. STABILITY ANALYSIS

In this section the stability of uniform solutions of Eqs. (35), (51), and (57) with respect to small perturbations is analyzed, where Eq. (51) is rewritten as

$$\tau_2\frac{\partial u_x}{\partial \xi}=-u_x+\gamma\frac{\partial}{\partial \eta}(|w|^2), \tag{67}$$

$$\tau_2\frac{\partial u_y}{\partial \xi}=-u_y+\gamma\frac{\partial}{\partial \zeta}(|w|^2). \tag{68}$$

If we write the complex amplitude w in the form

$$w=A\exp(i\Theta), \tag{69}$$

where $A=A(\xi,\eta,\zeta)$ and $\Theta=\Theta(\xi,\eta,\zeta)$ are real functions, we obtain

$$-A\frac{\partial\Theta}{\partial\xi}=\frac{\partial^2 A}{\partial\eta^2}+\frac{\partial^2 A}{\partial\zeta^2}-A\left[\left(\frac{\partial\Theta}{\partial\eta}\right)^2+\left(\frac{\partial\Theta}{\partial\zeta}\right)^2\right]+An, \tag{70}$$

$$\frac{\partial A}{\partial\xi}=2\left(\frac{\partial A}{\partial\eta}\frac{\partial\Theta}{\partial\eta}+\frac{\partial A}{\partial\zeta}\frac{\partial\Theta}{\partial\zeta}\right)+A\left(\frac{\partial^2\Theta}{\partial\eta^2}+\frac{\partial^2\Theta}{\partial\zeta^2}\right), \tag{71}$$

$$\frac{\partial n}{\partial\xi}=-\frac{\partial(nu_x)}{\partial\eta}-\frac{\partial(nu_y)}{\partial\zeta}-\frac{n-f(A^2)}{\tau_1}, \tag{72}$$

$$\tau_2\frac{\partial u_x}{\partial\xi}=-u_x+\gamma\frac{\partial A^2}{\partial\eta}, \tag{73}$$

$$\tau_2\frac{\partial u_y}{\partial\xi}=-u_y+\gamma\frac{\partial A^2}{\partial\zeta}. \tag{74}$$

It is easy to verify that

$$A=A_0=\text{const},\quad n=f(A_0^2),\ \ \Theta=-f(A_0^2)\xi,$$
$$u_x=0,\ \ u_y=0 \tag{75}$$

is a uniform solution of this system. The evolution of a small perturbation of this uniform solution

$$A=A_0+\tilde{A},\quad \Theta=-f(A_0^2)\xi+\tilde{\Theta},\quad n=f(A_0^2)+\tilde{n},$$
$$u_x=\tilde{u}_x, u_y=\tilde{u}_y \tag{76}$$

is given by the linearized equations

$$0=A_0\frac{\partial\tilde{\Theta}}{\partial\xi}+\frac{\partial^2\tilde{A}}{\partial\eta^2}+\frac{\partial^2\tilde{A}}{\partial\zeta^2}+A_0\tilde{n}, \tag{77}$$

$$0=\frac{\partial\tilde{A}}{\partial\xi}-A_0\left(\frac{\partial^2\tilde{\Theta}}{\partial\eta^2}+\frac{\partial^2\tilde{\Theta}}{\partial\zeta^2}\right), \tag{78}$$

$$0=\frac{\partial\tilde{n}}{\partial\xi}+f(A_0^2)\left(\frac{\partial\tilde{u}_x}{\partial\eta}+\frac{\partial\tilde{u}_y}{\partial\zeta}\right)+\frac{1}{\tau_1}[\tilde{n}-2A_0f'(A_0^2)\tilde{A}], \tag{79}$$

$$0=\tau_2\frac{\partial\tilde{u}_x}{\partial\xi}+\tilde{u}_x-2\gamma A_0\frac{\partial\tilde{A}}{\partial\eta}, \tag{80}$$

$$0=\tau_2\frac{\partial\tilde{u}_y}{\partial\xi}+\tilde{u}_y-2\gamma A_0\frac{\partial\tilde{A}}{\partial\zeta}. \tag{81}$$

Now let us consider the evolution of a periodic perturbation that can be written as

$$\begin{pmatrix}\tilde{A}\\ \tilde{\Theta}\\ \tilde{n}\\ \tilde{u}_x\\ \tilde{u}_y\end{pmatrix}=\begin{pmatrix}\hat{A}_1\\ \hat{\Theta}_1\\ \hat{n}_1\\ \hat{u}_x\\ \hat{u}_y\end{pmatrix}\exp(\sigma\xi+iK_x\eta+iK_y\zeta). \tag{82}$$

The stability of the uniform solution depends on the sign of the real part of the growth rate coefficient σ. In order to compute σ we substitute the perturbation Eq. (82) into the linearized Eqs. (77)–(81) and thus obtain the polynomial in σ,

$$f(\sigma)=a_4\sigma^4+a_3\sigma^3+a_2\sigma^2+a_1\sigma+a_0, \tag{83}$$

with

$$a_0=|\mathbf{K}|^4-2A_0^2|\mathbf{K}|^2[f'(A_0^2)+\tau_1\gamma f(A_0^2)|\mathbf{K}|^2], \tag{84}$$

$$a_1=(\tau_1+\tau_2)|\mathbf{K}|^4-2\tau_2A_0^2f'(A_0^2)|\mathbf{K}|^2, \tag{85}$$

$$a_2=1+\tau_1\tau_2|\mathbf{K}|^4, \tag{86}$$

$$a_3=\tau_1+\tau_2, \tag{87}$$

$$a_4=\tau_1\tau_2, \quad |\mathbf{K}|^2=K_x^2+K_y^2. \tag{88}$$

According to the Hurwitz criterion all roots σ of this polynomial possess negative real parts if and only if the following quantities are positive:

$$D_0=a_0, \tag{89}$$

$$D_1=a_1, \tag{90}$$

$$D_2=a_1a_2-a_0a_3, \tag{91}$$

$$D_3=a_3D_2-a_1^2a_4, \tag{92}$$

$$D_4=a_4D_3. \tag{93}$$

The analysis of this set of stability conditions gives us two types of instabilities.

(i) The inequality $D_0>0$ implies that for

$$A_0^2>A_*^2, \ A_*^2f(A_*{}^2)=\frac{1}{2\tau_1\gamma}, \tag{94}$$

perturbations with arbitrary wave length are unstable. For perturbations with $A_0<A_*$ the following stability criterion holds:

$$|\mathbf{K}|^2>K_*^2=\frac{2A_0^2f'(A_0^2)}{1-2\tau_1\gamma A_0^2f(A_0^2)}. \tag{95}$$

The inequality $D_1>0$ yields another stability condition

$$|\mathbf{K}|^2>K_{**}^2=\frac{2A_0^2f'(A_0^2)}{1+\tau_1/\tau_2}. \tag{96}$$

Since $K_*>K_{**}$ one obtains the long-wavelength instability criterion

$$|\mathbf{K}|<K_*. \tag{97}$$

This long-wavelength instability is more complicated that in the case of the (ordinary) nonlinear Schrödinger equation. In Fig. 2 the squares of the threshold values K_*^2 and K_{**}^2 are plotted versus the square of the amplitude A_0^2.

(ii) It is easy to see that, since $a_4>0$ and $a_3>0$, the set of conditions $D_2>0$, $D_3>0$, and $D_4>0$ is equivalent to the condition for stability

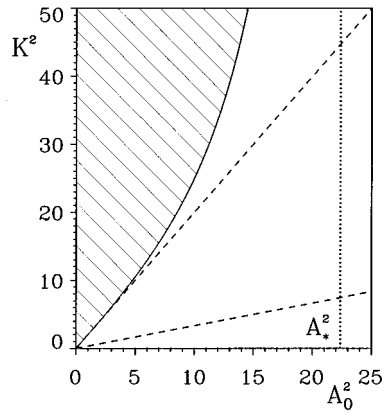

FIG. 2. Diagram for the instability of the first type for $\tau_1=0.1$, $\tau_2=0.02$, $\gamma=0.01$, and $A_\infty\to\infty$. The solid line shows the critical perturbation wave number K_* [Eq. (95)] and the shaded area gives the region of stability. The upper and the lower dashed lines give the stability threshold for the nonlinear Schrödinger equation (60) and the other critical perturbation wave number K_{**} [Eq. (96)], respectively. The threshold amplitude value equal A_* [Eq. (94)] is shown by the vertical dotted line.

$$D_2>\frac{a_1^2a_4}{a_3}, \tag{98}$$

which may be represented in the form

$$g(|\mathbf{K}|^2)=b_0-b_1|\mathbf{K}|^2+b_2|\mathbf{K}|^4>0, \tag{99}$$

with

$$b_0=(\tau_1+\tau_2)f'(A_0^2), \tag{100}$$

$$b_1=2\tau_2^3A_0^2f'^2(A_0^2)-\gamma(\tau_1+\tau_2)^2f(A_0^2), \tag{101}$$

$$b_2=\tau_2^2(\tau_1+\tau_2)f'^2(A_0^2). \tag{102}$$

For the case $b_1<0$ perturbations with arbitrary wave number $|\mathbf{K}|$ are stable. Thus the instability of the second type occurs only for $b_1>0$. For $A_\infty\to\infty$ [see Eq. (57)] this leads to the following stability criterion for waves with arbitrary wavelength

$$A_0^2<A_{**}^2=\frac{2\tau_2(\tau_1+\tau_2)}{2\tau_2^3-\gamma(\tau_1+\tau_2)^2}. \tag{103}$$

For $A_0>A_{**}$ inequality (99) gives the instability condition

$$K_-<|\mathbf{K}|<K_+, \tag{104}$$

where K_- and K_+ are the roots of equation $g(|\mathbf{K}|^2)=0$. The asymptotic formulas for K_+ and K_- for $A_0\to\infty$ are

$$K_+^2\to\frac{2\tau_2^3-\gamma(\tau_1+\tau_2)^2}{\tau_2^2(\tau_1+\tau_2)}A_0^2, \ K_-^2\to0. \tag{105}$$

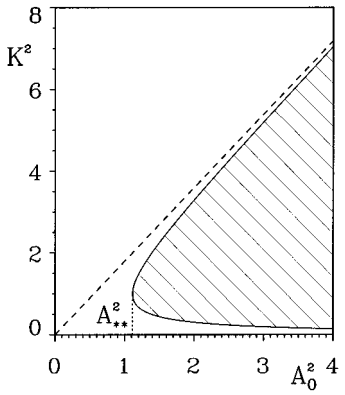

FIG. 3. Diagram for the instability of the second type for $\tau_1=0.1$, $\tau_2=1$, $\gamma=0.02$, and $A_\infty\to\infty$. The shaded area shows the region of instability and the dashed line gives the asymtotic behavior for K_+^2 [see Eq. (105)].

These results of the stability analysis are illustrated by the stability diagram of the $|\mathbf{K}|^2$–A_0^2 plane shown in Fig. 3. The long-wavelength instability may be interpreted as the reason for the occurrence of nonlinear structures, which will be discussed in the next section.

VI. RESULTS OF NUMERICAL SIMULATIONS

In this section we present results of numerical simulations using Eqs. (57), (51), and (35) for the evolution of the bubble concentration, velocity of bubbles, and the amplitude of the sound field, respectively. We have simulated the evolution of small perturbations of acoustic waves propagating along a channel with reflecting boundaries.

Our model contains four significant dimensionless parameters τ_1, τ_2, γ, and A_∞. The parameter τ_1 is the time of dissolution of microbubbles, τ_2 is the relaxation time of the velocity of the bubbles, γ is the characteristic parameter of the primary Bjerknes force, and A_∞ is a characteristic amplitude for the saturation of the generation of bubbles by the sound field.

Let us start from the one-dimensional (1D) case ($\partial/\partial\zeta=0$). The numerical algorithm used for solving our system of partial differential equations is presented in Appendix A. The initial condition consists of a uniform distribution of the amplitude of the acoustic field and the concentration of bubbles that is perturbed by a cosine function with small amplitude. For simplicity we investigate only perturbations with a wavelength equal to the distance between the lateral walls of the channel, which is given by

$$w(0,\eta)=w_0\left[1+\frac{w_1}{2}[1-\cos(\eta)]\right],$$

$$n(0,\eta)=|w(0,\eta)|^2,\quad u_x(0,\eta)=0, \tag{106}$$

with $w_0=1$ and $w_1=0.1$ (i.e., the case $K_x=1$, $\eta\in[0,2\pi]$). The spatial grid consisted of 257 points and the size of the time steps was $\Delta\xi=0.1(\Delta\eta)^2$ with $\Delta\eta=2\pi/256$. In the following figures the spatial interval has been normalized by 2π to $[0,1]$.

The systematic investigation of the influence of τ_1 and γ on the evolution of structures in the 1D case for $\tau_2=0$ (i.e., without added mass forces), $A_\infty\to\infty$, and $\gamma<0$ was carried out in [30]. Here we consider the influence of the parameters τ_2 and $\gamma>0$ on the structure formation for $A_\infty\to\infty$.

The evolution of small perturbations of the acoustic field given by Eqs. (106) for $\tau_1=0.1$, $\tau_2=0.02$, and $\gamma=0.01$ is presented in Fig. 4. The development of long-wavelength instability of the first type leads to the structure formation shown. (For this set of parameters the instability of the second type does not occur.) It is visible that the sound field amplitude $|w|$ does not exceed the instability threshold value A_*^2 given in Eq. (94). Therefore, this structure looks stable. The comparison of the shape of this structure with the classical soliton solution of the nonlinear Schrödinger equation is shown in Fig. 4(d).

These results agree qualitatively with the results of Ref. [30]. However, after a long time ($t>3700$) the position of this structure becomes unstable and the structure jumps to the wall of the channel, as shown in Fig. 5 for the bubble concentration n.

The influence of γ on the shape of this quasistable structure is shown in Fig. 6(a). For $\gamma\to0$ the shape of the quasistable structure converges to the stationary solution of the nonlinear Schrödinger equation. For increasing γ the primary Bjerknes force becomes stronger and therefore the width of the structure decreases. Furthermore, the amplitude of the structure increases and for sufficiently large γ exceeds the instability threshold Eq. (94).

The dependence of the transient oscillations of the maximum of the sound field amplitude $|w|$ is shown in Fig. 6(b). For $\tau_1\to0$ the behavior of the solution is quite similar to the periodic oscillations of the nonlinear Schrödinger equation [30]. If τ_1 is increased the oscillations are more strongly damped and the amplitude of the quasistable structure becomes larger.

Now let us consider the 2D case. The numerical algorithm used is given in Appendix B. The initial condition consists of a uniform distribution of the amplitude of the acoustic field and the concentration of bubbles that is perturbed by a cosine function with small amplitude for both directions (η and ζ). For simplicity we consider a channel with a quadratic cross section and investigate only perturbations with a wavelength equal to the distance between the lateral walls of the channel given by

$$w(0,\eta,\zeta)=w_0\left[1+\frac{w_1}{4}[1-\cos(\eta)][1-\cos(\zeta)]\right], \tag{107}$$

$$n(0,\eta,\zeta)=|w(0,\eta,\zeta)|^2,$$

$$u_x(0,\eta,\zeta)=0,\quad u_y(0,\eta,\zeta)=0,$$

with $w_0=1$ and $w_1=0.1$ (i.e., the case $K_x=1$, $K_y=1$, $\eta\in[0,2\pi]$, and $\zeta\in[0,2\pi]$). The spatial grid consisted of 257 points in each direction and the size of the time steps was $\Delta\xi=0.1(\Delta\eta)^2$ with $\Delta\eta=\Delta\zeta=2\pi/256$.

For the nonlinear Schrödinger equation in the 2D case a ''blowup'' phenomenon takes place and the formation of a solitonlike structure is impossible. The same blowup may

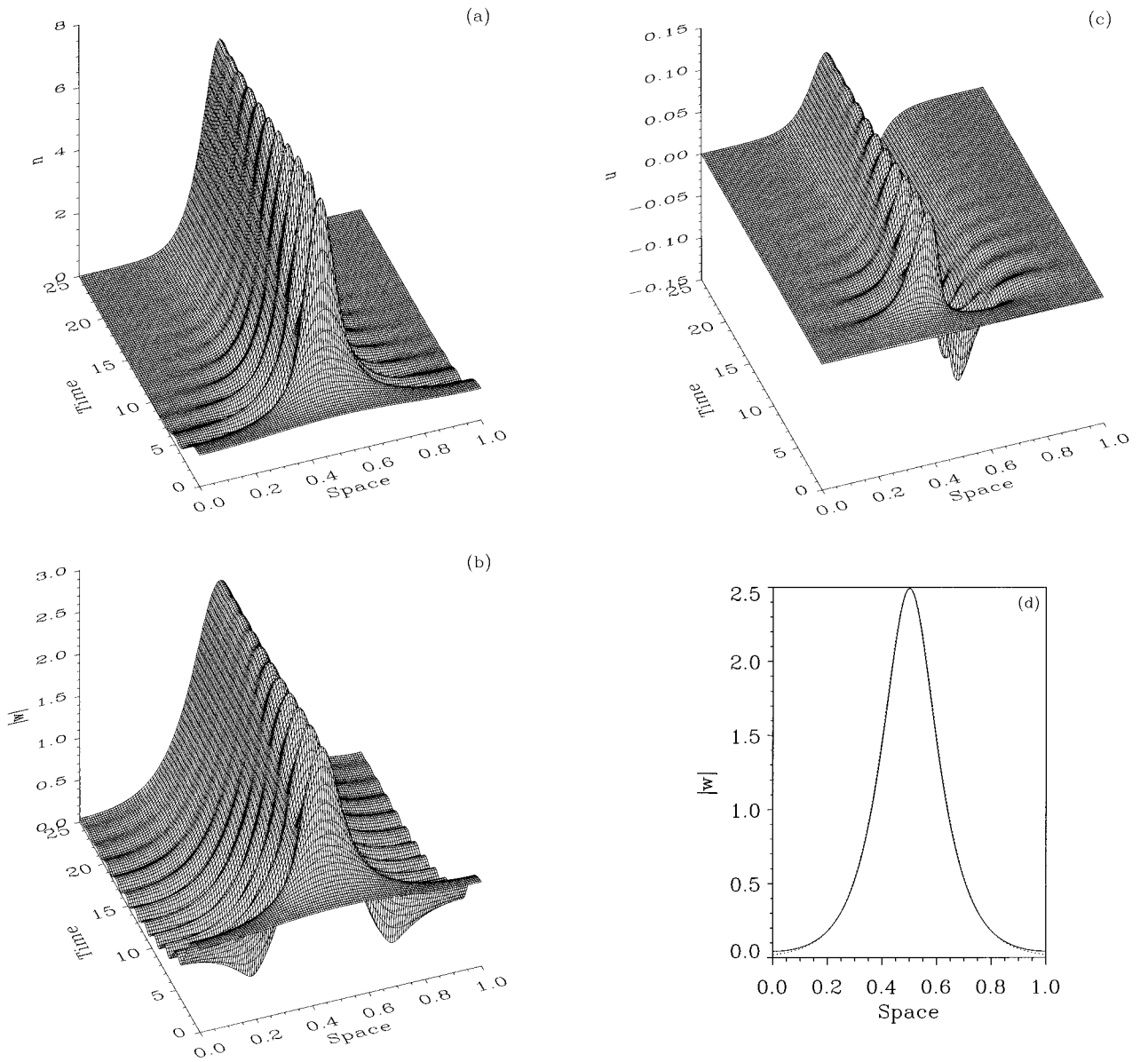

FIG. 4. Transient to the quasistable solitonlike structure in the one-dimensional case for $\tau_1=0.1$, $\tau_2=0.02$, $\gamma=0.01$, and $A_\infty\to\infty$. (a) Evolution of the bubble concentration n. (b) Evolution of the amplitude of the sound field $|w|$. (c) Evolution of the velocity of the bubbles u_x. (d) Comparison of the shape of the quasistable structure with the shape of a soliton solution of the nonlinear Schrödinger equation (dotted line).

occur in our model as illustrated in Fig. 7(a), where the maximum $|w|_{\max}$ of the sound field amplitude is plotted versus time. The blowup phenomenon may be stopped by the saturation of the bubble generation due to the limited amount of diluted gas. Such a saturation was modeled in Eq. (57) using a dimensionless saturation amplitude A_∞. For $A_\infty=2$ the blowup is stopped and we obtain, for small Bjerknes forces ($\gamma=0.001$), the evolution shown in Fig. 7(b). During the transient ($0<t<120$) a quasistable structure is generated in the center of the square. This can also be seen in Figs. 8(a)-8(c) where the corresponding pattern formation is shown. However, like in the 1D case (see Fig. 5) the position of this structure is not stable and therefore it starts, at $t\approx 130$, to move to the boundary (see Fig. 8). Because of this collision the amplitude $|w|_{\max}$ grows, as shown in Fig. 7(b). For larger Bjerknes forces ($\gamma>0.001$) the saturation level A_∞ is not small enough to stop the blowup phenomenon.

VII. DISCUSSION

A model for the theoretical description of a possible mechanism of pattern formation in acoustic cavitation is developed. It consists of an equation for the evolution of the bubble concentration in an acoustic field [Eq. (57)], an equation for the motion of bubbles in the acoustic field [Eq. (51)], and a nonlinear Schrödinger equation for the amplitude of the acoustic field [Eq. (35)], where the potential is replaced by the distribution of bubbles. Linear stability analysis of uniform configurations of bubbles shows a long-wavelength instability. The latter is quite similar to the long-wavelength instability for the nonlinear Schrödinger equation and may be interpreted as the reason for nonlinear structure formation.

Numerical simulations for the 1D and the 2D case show a ''self-concentration'' of bubbles in the sound field yielding localized (quasistable) solitonlike structures. These struc-

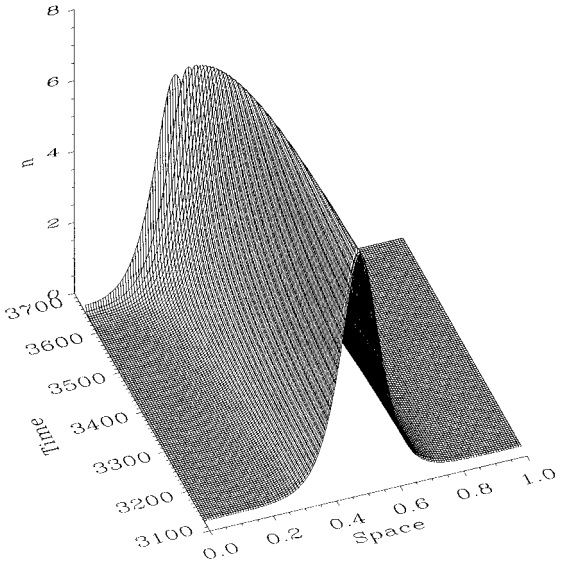

FIG. 5. Positional instability of the solitonlike structure in the one-dimensional case for $\tau_1=0.1$, $\tau_2=0.02$, $\gamma=0.01$, and $A_\infty\to\infty$.

tures may be interpreted as a first step towards the formation of streamers.

Future development of this approach should take into account secondary Bjerknes forces, rectified diffusion, coalescence and destruction of bubbles of different sizes, the presence of vapor in the bubbles, the nonlinear character of bubble oscillations, and the whole spatial pattern. Furthermore, in order to compare the theoretical approach with the experimental results (see Fig. 1 and [7]) it is necessary to consider the case of standing waves.

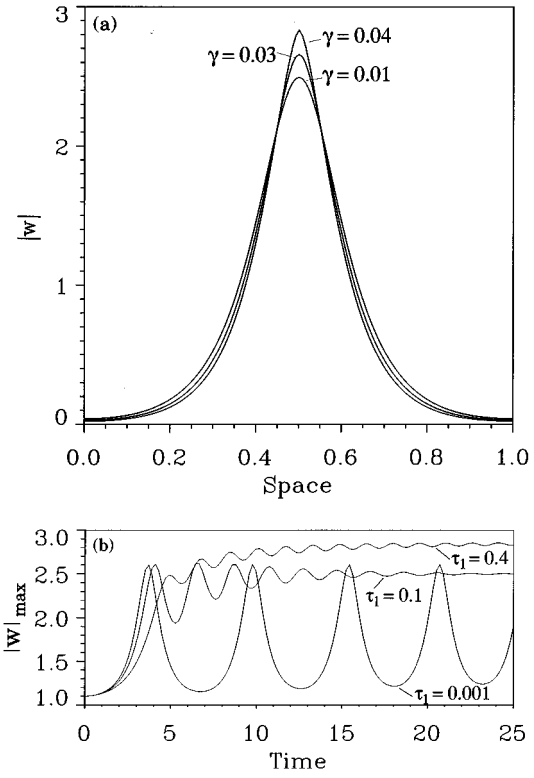

FIG. 6. (a) Dependence of the shape of the one-dimensional quasistable solitonlike structure on γ for $\tau_1=0.1$, $\tau_2=0.02$, and $A_\infty\to\infty$. (b) Evolution of the maxima of the amplitude of the acoustic field during the transient to the one-dimensional quasistable structure for $\gamma=0.01$, $\tau_2=0.02$, $A_\infty\to\infty$, and different values of τ_1.

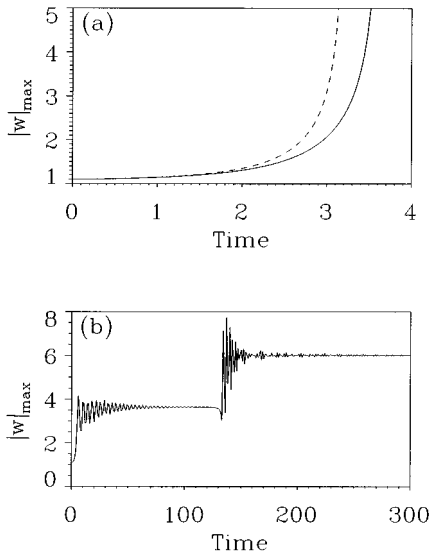

FIG. 7. Evolution of the maxima of the amplitude of the acoustic field for the two-dimensional case. (a) Blowup phenomenon for $\tau_1=0.1$, $\tau_2=0.02$, $\gamma=0.01$, and $A_\infty\to\infty$ (solid line) and a comparison with the solution of the nonlinear Schrödinger equation (dashed line). (b) Evolution of the maxima of the amplitude of the acoustic field during the transient to the quasistable structure for $\tau_1=0.1$, $\tau_2=0.02$, $\gamma=0.001$, and $A_\infty=2$ with a jump due to the positional instability.

ACKNOWLEDGMENTS

This work was supported by the Deutsche Forschungsgemeinschaft (Sonderforschungsbereich 185–Nonlinear Dynamics), the Stabsstelle für Internationale Beziehungen (Contract No. X222.31), the Ministry for Science, Higher Education and Technical Policy of the Russian Federation, and the State Committee of the Russian Federation for Higher Education.

APPENDIX A: NUMERICAL METHOD FOR THE 1D CASE

In this appendix we discuss the numerical scheme for solving the system of partial differential equations

$$i\frac{\partial w}{\partial t}=\frac{\partial^2 w}{\partial x^2}+nw, \tag{A1}$$

$$\frac{\partial n}{\partial t}+\frac{\partial (nu)}{\partial x}=-\frac{n-f(|w|^2)}{\tau_1}, \tag{A2}$$

$$\tau_2\frac{\partial u}{\partial t}+u=-\gamma\frac{\partial}{\partial x}(|w|^2), \tag{A3}$$

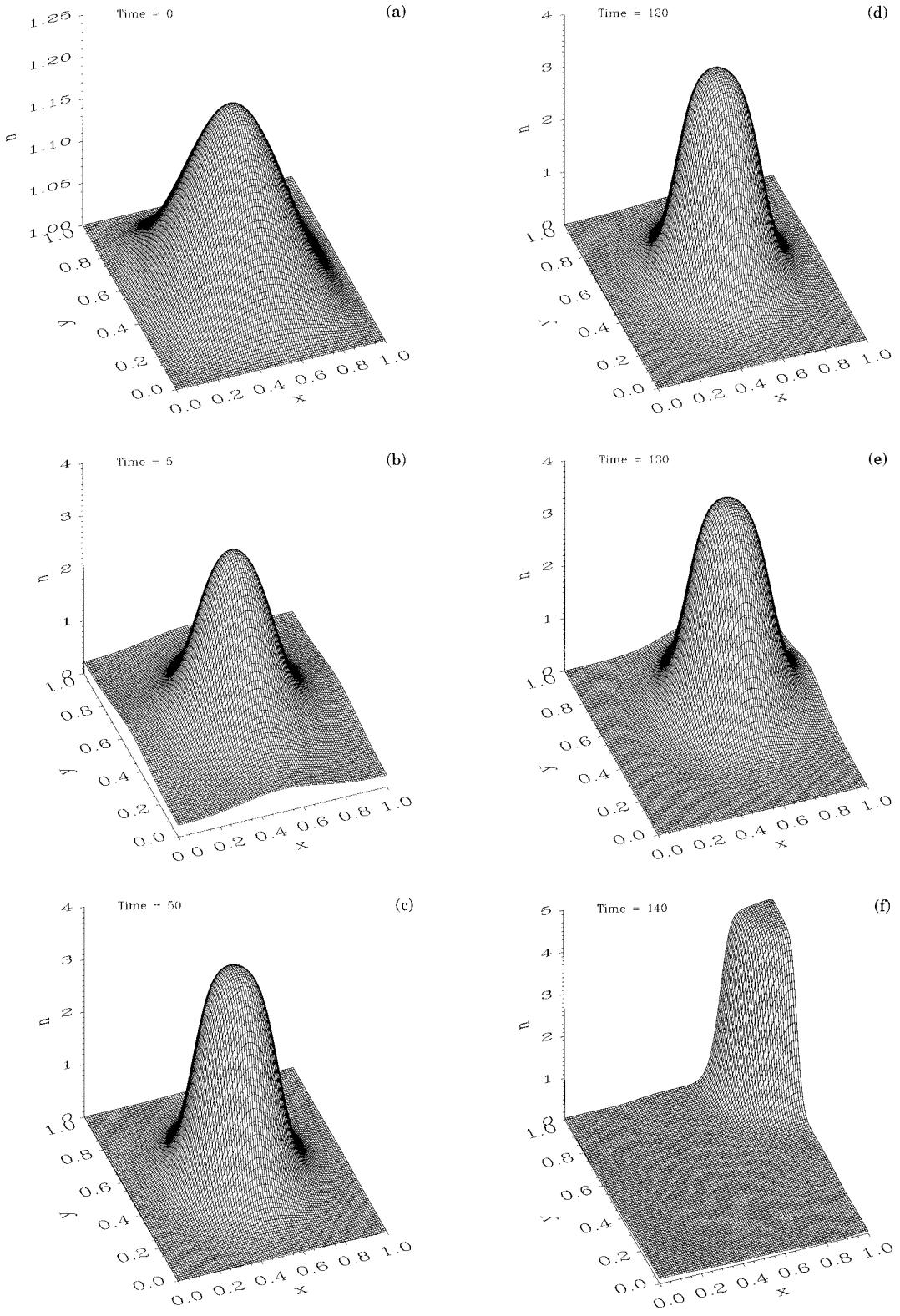

FIG. 8. Structure formation and the development of the positional instability for $\tau_1=0.1$, $\tau_2=0.02$, $\gamma=0.001$, and $A_\infty=2$.

for $0<x<L$ and $t>0$. (Here we use the standard variables x and t for space and time and the velocity component u_x is replaced by u to obtain formulas that are more readable.) For solving the amplitude equation (A1) a Crank-Nicholson scheme for the linear Schrödinger equation [38,39] was modified for the nonlinear case

$$i\frac{w_j^{n+1}-w_j^n}{\Delta t}=\frac{1}{2(\Delta x)^2}[w_{j-1}^{n+1}-2w_j^{n+1}+w_{j+1}^{n+1}+w_{j-1}^n-2w_j^n+w_{j+1}^n]+\frac{1}{2}(n_j^n w_j^n+n_j^{n+1}w_j^{n+1}), \tag{A4}$$

where $w_j^n=w(x_j,t_n)$, $n_j^n=n(x_j,t_n)$, $x_j=(j-1)\Delta x$, and $t_n=n\Delta t$ with $j=1,\ldots,J$ and $n=0,1,2,\ldots$. For numerical computations it is necessary to rewrite this system of linear equations in tridiagonal form

$$w_{j-1}^{n+1}+B_j^n w_j^{n+1}+w_{j+1}^{n+1}=R_j^n, \tag{A5}$$

with

$$B_j^n=-2-a_1+a_2 n_j^{n+1}, \tag{A6}$$

$$R_j^n=-w_{j+1}^n-w_{j-1}^n+(2-a_1-a_2 n_j^n)w_j^n, \tag{A7}$$

where

$$a_1=\frac{2(\Delta x)^2 i}{\Delta t}, \quad a_2=(\Delta x)^2, \tag{A8}$$

and $j=2,\ldots,J-1$. The boundary condition Eq. (61) can be approximated by $w_1^{n+1}=w_2^{n+1}$ and $w_J^{n+1}=w_{J-1}^{n+1}$. For solving Eq. (A1) for the bubble concentration n we used the discretization scheme

$$\frac{n_j^{n+1}-n_j^{n-1}}{2\Delta t}+\frac{n_{j+1}^n u_{j+1}^n-n_{j-1}^n u_{j-1}^n}{2\Delta x}+\frac{n_j^{n+1}+n_j^{n-1}}{2\tau_1}-\frac{f(|w_j^n|^2)}{\tau_1}=0 \tag{A9}$$

for $j=2,\ldots,J-1$. This can be rewritten as an explicit scheme that may be considered as a modified ''staggered leapfrog'' method [39]:

$$n_j^{n+1}=b_1 n_j^{n-1}-b_2(n_{j+1}^n u_{j+1}^n-n_{j-1}^n u_{j-1}^n)+b_3 f(|w_j^n|^2), \tag{A10}$$

with

$$b_1=\frac{\tau_1-\Delta t}{\tau_1+\Delta t}, \quad b_2=\frac{\tau_1\Delta t}{(\tau_1+\Delta t)\Delta x}, \quad b_3=\frac{2\Delta t}{\tau_1+\Delta t}. \tag{A11}$$

At the bondaries we use mirror reflection boundary conditions

$$u_0=-u_2, \quad n_0=n_2, \quad u_{J+1}=-u_{J-1}, \quad n_{J+1}=n_{J-1}, \tag{A12}$$

which yield equations for the boundary values

$$n_1^{n+1}=b_1 n_1^{n-1}-2b_2 n_2^n u_2^n+b_3 f(|w_1^n|^2), \tag{A13}$$

$$n_J^{n+1}=b_1 n_J^{n-1}+2b_2 n_{J-1}^n u_{J-1}^n+b_3 f(|w_J^n|^2). \tag{A14}$$

The integration scheme for the velocity u is also a modified staggered leapfrog method [39] and is given by the discretization

$$\tau_2\frac{u_j^{n+1}-u_j^{n-1}}{2\Delta t}+\frac{1}{2}(u_j^{n+1}+u_j^{n-1})+\frac{\gamma}{2\Delta x}(|w_{j+1}^n|^2-|w_{j-1}^n|^2)=0 \tag{A15}$$

or explicitly formulated,

$$u_j^{n+1}=c_1 u_j^{n-1}-c_2(|w_{j+1}^n|^2-|w_{j-1}^n|^2), \tag{A16}$$

with

$$c_1=\frac{\tau_2-\Delta t}{\tau_2+\Delta t}, \quad c_2=\frac{\gamma\Delta t}{(\tau_2+\Delta t)\Delta x}, \tag{A17}$$

and $j=2,\ldots,J-1$. The boundary conditions are

$$u_1^{n+1}=0=u_J^{n+1}. \tag{A18}$$

They are obtained by substituting in Eq. (A3) the boundary conditions (61) for w and the initial condition $u(x,0)=0$.

APPENDIX B: NUMERICAL METHOD FOR THE 2D CASE

In this appendix we discuss the numerical scheme for solving the system of partial differential equations

$$i\frac{\partial w}{\partial t}=\frac{\partial^2 w}{\partial x^2}+\frac{\partial^2 w}{\partial y^2}+nw, \tag{B1}$$

$$\frac{\partial n}{\partial t}+\frac{\partial(nu)}{\partial x}+\frac{\partial(nv)}{\partial y}=-\frac{n-f(|w|^2)}{\tau_1}, \tag{B2}$$

$$\tau_2\frac{\partial u}{\partial t}+u=-\gamma\frac{\partial}{\partial x}(|w|^2), \tag{B3}$$

$$\tau_2\frac{\partial v}{\partial t}+v=-\gamma\frac{\partial}{\partial y}(|w|^2) \tag{B4}$$

for $0<x<L$, $0<y<L$, and $t>0$. (Here we use the standard variables x, y, and t for space and time and the velocity components u_x and u_y are replaced by u and v.) For the approximation of Eq. (B1) between the time levels n and $n+1$ we use the approximation of n,

$$\tilde{n}_{j,k}^n=\frac{n_{j,k}^n+n_{j,k}^{n+1}}{2}. \tag{B5}$$

The equation for w is solved using an alternating-direction implicit method [39]. The first substep is given by

$$i\frac{w_{j,k}^{n+1/2}-w_{j,k}^n}{\Delta t/2}=\frac{w_{j-1,k}^{n+1/2}-2w_{j,k}^{n+1/2}+w_{j+1,k}^{n+1/2}}{\Delta^2}+\frac{w_{j,k-1}^n-2w_{j,k}^n+w_{j,k+1}^n}{\Delta^2}+\frac{n_{j,k}^n+n_{j,k}^{n+1}}{2}\frac{w_{j,k}^n+w_{j,k}^{n+1/2}}{2} \tag{B6}$$

for $j=2,\ldots,J-1$, where $w_{j,k}^n=w(x_j,y_k,t_n)$, $n_{j,k}^n=n(x_j,y_k,t_n)$, $x_j=(j-1)\Delta$, $y_k=(k-1)\Delta$, and $t_n=n\Delta t$ with $j=1,\ldots,J$, $k=1,\ldots,K$, $J=K$, and $n=0,1,2,\ldots$. In tridiagonal form this equation reads

$$w_{j-1,k}^{n+1/2}+B_{j,k}^n w_{j,k}^{n+1/2}+w_{j+1,k}^{n+1/2}=R_{j,k}^n, \tag{B7}$$

with

$$B_{j,k}^{n}=-2-a_1+a_2(n_{j,k}^{n}+n_{j,k}^{n+1}), \tag{B8}$$

$$R_{j,k}^{n}=-w_{j,k-1}^{n}-w_{j,k+1}^{n}+[2-a_1-a_2(n_{j,k}^{n}+n_{j,k}^{n+1})]w_{j,k}^{n}, \tag{B9}$$

where

$$a_1=\frac{2\Delta^2 i}{\Delta t}, \quad a_2=\frac{\Delta^2}{4} \tag{B10}$$

and $j=2,\ldots,J-1$. The second substep is given by

$$i\frac{w_{j,k}^{n+1}-w_{j,k}^{n+1/2}}{\Delta t/2}=\frac{w_{j-1,k}^{n+1/2}-2w_{j,k}^{n+1/2}+w_{j+1,k}^{n+1/2}}{\Delta^2}+\frac{w_{j,k-1}^{n+1}-2w_{j,k}^{n+1}+w_{j,k+1}^{n+1}}{\Delta^2}+\frac{n_{j,k}^{n}+n_{j,k}^{n+1}}{2}\,\frac{w_{j,k}^{n+1/2}+w_{j,k}^{n+1}}{2} \tag{B11}$$

for $k=2,\ldots,K-1$. In tridiagonal form this equation reads

$$w_{j,k-1}^{n+1}+B_{j,k}^{n+1/2}w_{j,k}^{n+1}+w_{j,k+1}^{n+1}=R_{j,k}^{n+1/2}, \tag{B12}$$

with

$$B_{j,k}^{n+1/2}=-2-a_1+a_2(n_{j,k}^{n}+n_{j,k}^{n+1}), \tag{B13}$$

$$R_{j,k}^{n+1/2}=-w_{j-1,k}^{n+1/2}-w_{j+1,k}^{n+1/2}+[2-a_1-a_2(n_{j,k}^{n}+n_{j,k}^{n+1})]w_{j,k}^{n+1/2}, \tag{B14}$$

and $k=2,\ldots,K-1$.

The discretization scheme for Eq. (B2) describing the evolution of the bubble concentration n is given by

$$\frac{n_{j,k}^{n+1}-n_{j,k}^{n-1}}{2\Delta t}+\frac{n_{j+1,k}^{n}u_{j+1,k}^{n}-n_{j-1,k}^{n}u_{j-1,k}^{n}}{2\Delta x}+\frac{n_{j,k+1}^{n}v_{j,k+1}^{n}-n_{j,k-1}^{n}v_{j,k-1}^{n}}{2\Delta y}+\frac{1}{2\tau_1}(n_{j,k}^{n+1}+n_{j,k}^{n-1})-\frac{1}{\tau_1}f(|w_{j,k}^{n}|^2)=0 \tag{B15}$$

and the values of $n_{j,k}^{n+1}$ may be calculated explicitly as

$$n_{j,k}^{n+1}=b_1 n_{j,k}^{n-1}-b_2(n_{j+1,k}^{n}u_{j+1,k}^{n}-n_{j-1,k}^{n}u_{j-1,k}^{n}+n_{j,k+1}^{n}v_{j,k+1}^{n}-n_{j,k-1}^{n}v_{j,k-1}^{n})+b_3 f(|w_{j,k}^{n}|^2) \quad (j=2,\ldots,J-1;k=2,\ldots,K-1), \tag{B16}$$

with

$$b_1=\frac{\tau_1-\Delta t}{\tau_1+\Delta t}, \quad b_2=\frac{\tau_1\Delta t}{(\tau_1+\Delta t)\Delta}, \quad b_3=\frac{2\Delta t}{\tau_1+\Delta t}, \tag{B17}$$

and $j=2,\ldots,J-1$, $k=2,\ldots,K-1$. For n we use mirror reflection boundary conditions. Thus we obtain, for $k=2,\ldots,K-1$,

$$n_{1,k}^{n+1}=b_1 n_{1,k}^{n-1}-b_2(2n_{2,k}^{n}u_{2,k}^{n}+n_{1,k+1}^{n}v_{1,k+1}^{n}-n_{1,k-1}^{n}v_{1,k-1}^{n})+b_3 f(|w_{1,k}^{n}|^2), \tag{B18}$$

$$n_{J,k}^{n+1}=b_1 n_{J,k}^{n-1}-b_2(-2n_{J-1,k}^{n}u_{J-1,k}^{n}+n_{J,k+1}^{n}v_{J,k+1}^{n}-n_{J,k-1}^{n}v_{J,k-1}^{n})+b_3 f(|w_{J,k}^{n}|^2). \tag{B19}$$

Analogously we obtain, for $j=2,\ldots,J-1$,

$$n_{j,1}^{n+1}=b_1 n_{j,1}^{n-1}-b_2(n_{j+1,1}^{n}u_{j+1,1}^{n}-n_{j-1,1}^{n}u_{j-1,1}^{n}+2n_{j,2}^{n}v_{j,2}^{n})+b_3 f(|w_{j,1}^{n}|^2), \tag{B20}$$

$$n_{j,K}^{n+1}=b_1 n_{j,K}^{n-1}-b_2(n_{j+1,K}^{n}u_{j+1,K}^{n}-n_{j-1,K}^{n}u_{j-1,K}^{n}-2n_{j,K-1}^{n}v_{j,K-1}^{n})+b_3 f(|w_{j,K}^{n}|^2). \tag{B21}$$

At the corners we have

$$n_{1,1}^{n+1}=b_1 n_{1,1}^{n-1}-b_2(2n_{2,1}^{n}u_{2,1}^{n}+2n_{1,2}^{n}v_{1,2}^{n})+b_3 f(|w_{1,1}^{n}|^2), \tag{B22}$$

$$n_{1,K}^{n+1}=b_1 n_{1,K}^{n-1}-b_2(2n_{2,K}^{n}u_{2,K}^{n}-2n_{1,K-1}^{n}v_{1,K-1}^{n})+b_3 f(|w_{1,K}^{n}|^2), \tag{B23}$$

$$n_{J,1}^{n+1}=b_1 n_{J,1}^{n-1}-b_2(-2n_{J-1,1}^{n}u_{J-1,1}^{n}+2n_{J,2}^{n}v_{J,2}^{n})+b_3 f(|w_{J,1}^{n}|^2), \tag{B24}$$

$$n_{J,K}^{n+1}=b_1 n_{J,K}^{n-1}-b_2(-2n_{J-1,K}^{n}u_{J-1,K}^{n}-2n_{J,K-1}^{n}v_{J,K-1}^{n})+b_3 f(|w_{J,K}^{n}|^2). \tag{B25}$$

The equations for the velocities have been discretized as

$$\tau_2\frac{u_{j,k}^{n+1}-u_{j,k}^{n-1}}{2\Delta t}+\frac{1}{2}(u_{j,k}^{n+1}+u_{j,k}^{n-1})+\gamma\frac{|w_{j+1,k}^{n}|^2-|w_{j-1,k}^{n}|^2}{2\Delta}=0. \tag{B26}$$

The discretization (B26) yields the explicit scheme

$$u_{j,k}^{n+1}=c_1 u_{j,k}^{n-1}-c_2(|w_{j+1,k}^n|^2-|w_{j-1,k}^n|^2), \quad \text{(B27)}$$

for $j=2,\ldots,J-1$; $k=1,\ldots,K$ with boundary condition $u_{1,k}=u_{J,k}=0$ for $k=1,\ldots,K$ and

$$c_1=\frac{\tau_2-\Delta t}{\tau_2+\Delta t}, \quad c_2=\frac{\gamma\Delta t}{(\tau_2+\Delta t)\Delta}. \quad \text{(B28)}$$

Similarly we obtain, for the second component

$$\tau_2\frac{v_{j,k}^{n+1}-v_{j,k}^{n-1}}{2\Delta t}+\frac{1}{2}(v_{j,k}^{n+1}+v_{j,k}^{n-1})+\gamma\frac{|w_{j,k+1}^n|^2-|w_{j,k-1}^n|^2}{2\Delta}=0 \quad \text{(B29)}$$

or, explicitly,

$$v_{j,k}^{n+1}=c_1 v_{j,k}^{n-1}-c_2(|w_{j,k+1}^n|^2-|w_{j,k-1}^n|^2) \quad \text{(B30)}$$

for $k=2,\ldots,K-1$; $j=1,\ldots,J$ and at the boundary $v_{j,1}=v_{j,K}=0$ for $j=1,\ldots,J$.

[1] F.R. Young, *Cavitation* (McGraw-Hill, London, 1989).
[2] T.G. Leighton, *The Acoustic Bubble* (Academic, London, 1994).
[3] *Cavitation and Inhomogeneities in Underwater Acoustics*, edited by W. Lauterborn (Springer, Berlin, 1980).
[4] *Mechanics and Physics of Bubbles in Liquids*, edited by L. van Wijngaarden (Nijhoff, The Hague, 1982).
[5] *Bubble Dynamics and Interface Phenomena*, edited by J.R. Blake, J.M. Boulton-Stone, and N.H. Tomas (Kluwer Academic, Dordrecht, 1993).
[6] G.C. Lichtenberg, in *Novi Commentarii Societatis Regiae Scientiarum Gottingensis*, edited by J. C. Dieterich (Dieterich, Göttingen, 1778). pp. 168–180.
[7] W. Lauterborn, E. Schmitz, and A. Judt, Int. J. Bifurcation Chaos **3**, 635 (1993).
[8] S.V. Iordanskii, Prikl. Mekh. Tekhn. Fiz. **3**, 102 (1960).
[9] B.S. Kogarko, Dokl. Akad. Nauk SSSR **137**, (1961) [Sov. Phys. Dokl. **6**, 305 (1961)].
[10] G.K. Batchelor, Fluid Dyn. Trans. Warsaw **4**, 425 (1967).
[11] L. van Wijngaarden, Annu. Rev. Fluid Mech. **4**, 369 (1972).
[12] R.I. Nigmatulin, *Fundamentals of Mechanics of Heterogeneous Media* (Nauka, Moscow, 1987).
[13] R.I. Nigmatulin, *Dynamics of Multiphase Media* (Hemisphere, New York, 1991), Vols. 1 and 2.
[14] V.E. Nakoryakov, B.G. Pokusaev, and I.R. Shreiber, *Propagation of Waves in Gas-Liquid and Lapor-Liquid Media* (ITF, Novosibirsk, 1983).
[15] V.K. Kedrinskii, Prikl. Mekh. Tekh. Fiz. **4**, 29 (1968).
[16] V.Sh. Shagapov, Prikl. Mekh. Tekhn. Fiz. **18**, 90 (1977) [J. Appl. Mech. Tech. Phys. **18**, 77 (1977)]
[17] R.F. Ganiev and L.E. Ukrainskii, Prikl. Mekh. (USSR) **11**, 3 (1975) [Sov. Appl. Mech. **11**, 3 (1975)].
[18] R.F. Ganiev and V.F. Lapchinskii, *Problems of Mechanics in Cosmic Technology* (Mashinostroenie, Moscow, 1978).
[19] S.L. Gavrilyuk, Prikl. Mekh. Tekh. Fiz. **30**, 86 (1989) [J. Appl. Mech. Tech. Phys. **30**, 247 (1989)].
[20] N.A. Gumerov, J. Appl. Math. Mech. **56**, 50 (1992).
[21] L. van Wijngaarden, J. Fluid. Mech. **33**, 465 (1968).
[22] G. Iernetti and M.S. Sagoo, Acustica **41**, 32 (1978).
[23] P. Ciuti, G. Iernetti, and M.S. Sagoo, Ultrasonics, **18**, 111 (1980).
[24] I. Akhatov, V. Baikov, and R. Baikov, Izv. Akad. Nauk SSSR, Mekh. Zhidk. Gaza **1**, 180 (1986).
[25] I. Akhatov and V. Baikov, Inzh. Fiz. Zh. **50**, 385 (1986).
[26] N.A. Gumerov, in *Proceedings of the International Union of Theoretical and Applied Mechanics Symposium on Waves in Liquid/Gas and Liquid/Vapor Two-Phase Systems*, edited by S. Morioka and L. van Wijngarden (Kluwer Academic, Dordrecht, 1995), pp. 77–86.
[27] P. Smereka and S. Banerjee, Phys. Fluids **31**, 3519 (1988).
[28] L. D'Agostino and C.E. Brennen, J. Fluid Mech. **199**, 155 (1989).
[29] Y.A. Kobelev and L.A. Ostrovsky, J. Acoust. Soc. Am. **85**, 621 (1989).
[30] I. Akhatov, U. Parlitz, and W. Lauterborn, J. Acoust. Soc. Am. **96**, 3627 (1994). The parameter γ used in that paper corresponds to negative values of γ introduced in the present paper. Physically this means that the case of bubbles larger than the resonance radius was investigated in Ref. [30].
[31] U. Parlitz, C. Scheffczyk, I. Akhatov, and W. Lauterborn, Chaos Solitons Fractals **5**, 1881 (1995).
[32] I. Akhatov, U. Parlitz, and W. Lauterborn, in *Self-organization in Cavitation Bubble Fields*, Proceedings of the Second International Conference on Multiphase Flow, Kyoto, 1995, edited by A. Serizawa, T. Fukano, and J. Bataille (Japan Society of Multiphase Flow, Kyoto, 1995).
[33] V.F.J. Bjerknes, *Fields of Force* (Columbia University Press, New York, 1906).
[34] F.G. Blake, J. Acoust. Soc. Am. **21**, 551 (1949).
[35] A.J. Walton and G. T. Reynolds, Adv. Phys. **33**, 595 (1984).
[36] P.S. Epstein and M. S. Plesset, J. Chem. Phys. **18**, 1505 (1950).
[37] F.G. Blake, Harvard University, Acoustics Research Laboratory Report No. 12, 1949 (unpublished).
[38] A. Goldberg, H.M. Schey, and J.L. Schwartz, Am. J. Phys. **35**, 177 (1967).
[39] W.F. Ames, *Numerical Methods for Partial Differential Equations* (Academic, New York, 1977).